# Wind Stress Curl and Surface Circulation in the South China Sea and the Philippine Sea

**Charina Lyn A. Amedo[a]* and Cesar L. Villanoy[b]**
Marine Science Institute, College of Science
University of the Philippines Diliman
1101 Quezon City, Philippines
Telefax No.: (632) 922-3957
Email: [a]cla@upmsi.ph; [b]cesarv@upmsi.ph

## ABSTRACT

Wind stress curl is believed to be the main driving force for the circulation in the South China Sea. However, there has been no attempt to relate wind stress curl with surface currents. In this study, the variability of wind stress curl and surface currents were characterized using time-domain empirical orthogonal functions (EOF). The data used were the monthly average wind stress curl obtained from UWM COADS monthly time series for 1980-1989 and Richardson's ship-drift derived surface currents. Surface current EOF analysis yields three dominant modes, which account for 50%, 13%, and 7% of the total variance. Mode 1 is dominated by the western boundary current system in the Pacific with no significant temporal variations. Mode 2 reflects reversal of the South China Sea western boundary flow and variations in Mindanao eddy associated with the reversing monsoons. Mode 3 magnitudes were maximum during the monsoon transition periods and were dominated by the circulation in the Celebes Sea. For the wind stress curl, the first two EOF modes explained 40% and 32% of the total variance, respectively. Mode 1 is dominated by the positive wind stress curl throughout the South China Sea during the northeast monsoon. Mode 2 is associated with wind stress curl distribution during the southwest monsoon. The seasonal variability of surface currents in the South China Sea was highlighted by the seasonal reversal of the western boundary currents consistent with the reversal of the wind stress curl in the southern part of the South China Sea. In the interior, the surface currents were mostly associated with Ekman drift, except in the central part where an eastward extension of the western boundary current was observed during the southwest monsoon.

*Key words*: empirical orthogonal function, wind stress curl, South China Sea, surface currents

## INTRODUCTION

The South China Sea, located near the link of ocean-atmosphere circulation over the Indian Ocean and the Pacific Ocean (Fig. 1), is considered as one of the most important marginal seas for the world climate research community (He et al., 1987). The South China Sea has bottom topography that makes it a unique semi-enclosed ocean basin overlaid by a pronounced monsoon surface wind. The deepest water is confined to a bowl-type trench where the maximum depth is around 4,700 m (Chu et al., 1997). Situated within the strong influence of the monsoonal winds, it shows definite seasonal variations highly sensitive to the Asian monsoon. Seasonally, the surface circulation is cyclonic in winter

* *Corresponding author*

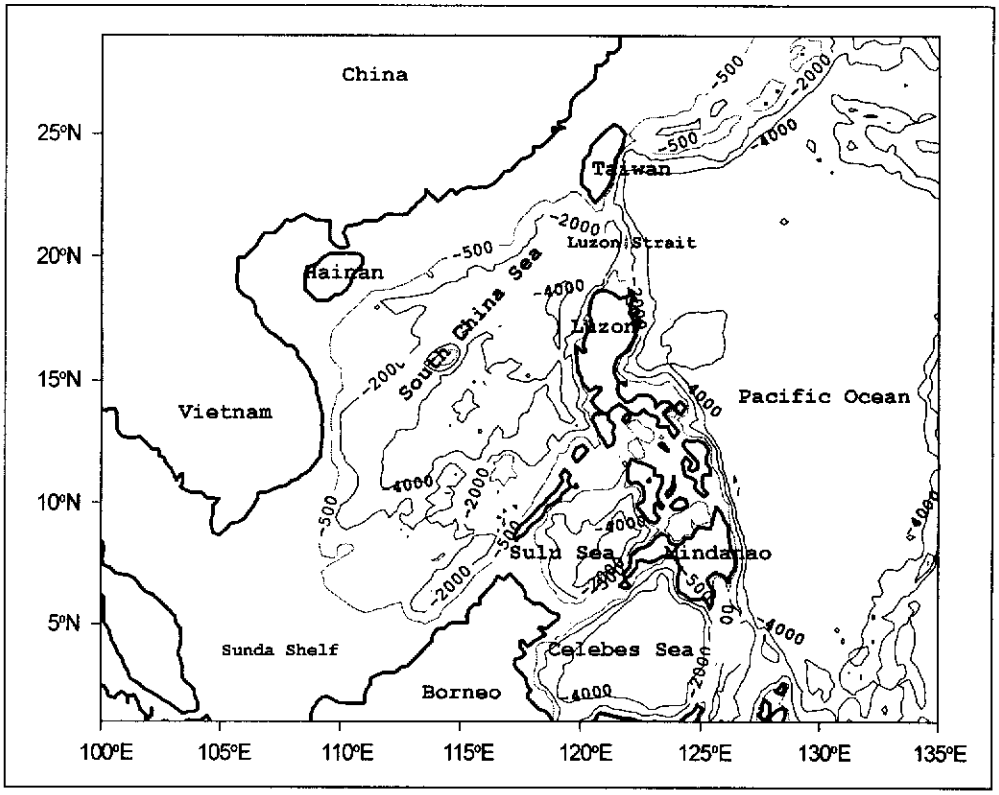


Fig. 1. Map of the South China Sea with -500 m, -2000 m, and -4000 m isobaths shown.

and anticyclonic in summer. Circulation is dominated by local wind forcing (Pohlman, 1987; Shaw et al., 1994; Chao et al., 1996), but it is not clear whether the wind stress or its curl is more important. Dynamically, the wind stress curl can either produce convergence or divergence in the surface currents in response to the horizontal gradient of sea surface height, which generates geostrophic current. On the other hand, observed surface drift currents contain both geostrophic flow and the Ekman flow. In terms of the role of wind stress on surface current, it is more important near the coast than in the open ocean. The flow in shallow water is essentially controlled by wind stress and bottom friction, whereas geostrophy and wind stress curl is significant in the open ocean.

Previous studies on the dynamics of circulation in the South China Sea inferred from sea surface height variations suggest that wind stress curl is the main driving force for the circulation in the deep basin except near the Luzon Strait (Shaw et al., 1999). The entire deep basin forming a cyclonic gyre and the shallow waters near the continental margin south of China are curl-driven. Both the change of the Coriolis parameter with latitude ($\beta$-effect) and the wind stress curl are essential to produce this basin-wide circulation in winter (Chao et al. (1996) and Stommel (1948) as cited by Shaw et al. (1999)). The formation of the West Luzon Eddy at about 18°N, 118°E northwest of Luzon and the East Vietnam Eddy located at about 14°N, 110°E are also due to both local wind stress curl and basin-scale circulation (Qu, 2000). In the summer, wind stress curl leads to the generation of a two-gyre circulation pattern with an eastward jet separating from the coast off central Vietnam. This pattern corresponds to the wind stress curl, which is negative to the south and positive to the north, with zero line running from southwest to northeast. The western boundary current, which separates from the coast off Vietnam following the line of zero wind stress curl, is well established in June and remains more or less stationary from June to August. This wind pattern reverses in December, with line of zero curls being farther north (Chao et al., 1996; Shaw et al., 1999; Qu, 2000). The formation of a gyre system in the eastern part (Qu, 2000) and the region west of the Luzon Strait, on the other hand, is better determined by the wind stress.

The objective of this study is to determine the variability of wind stress curl and the surface current field in the South China Sea and the western side of the Pacific. Previous studies relating wind forcing with surface dynamics in this area used velocity fields derived from models, or geostrophic calculations. This study attempts to relate wind stress curl with actual surface currents derived from ship's drift data.

## METHODOLOGY

The data used include the monthly wind stress obtained from UWM/COADS monthly series from 1980 to 1989 (http://ferret.wrc.noaa.gov/las/main.pl) and Richardson's ship-drift derived surface currents (http://ferret.wrc.noaa.gov/las/main.pl) available online. The wind stress curl was calculated from the corrected zonal and meridional wind stress using the equation:

$$curl(\tau) = \frac{\partial \tau_y}{\partial x} - \frac{\partial \tau_x}{\partial y}$$

where $\tau_y$ and $\tau_x$ are the $x$- and $y$-components of $\tau$.

The data were analyzed on a 1°x1° grid resolution within 1°-29°N and 95.5°-135°E. Monthly average of wind stress curl from ten years of marine observations and monthly mean historical surface current data were extracted. Both surface circulation and wind stress curl time series data were checked to ensure that there were no gaps in the time series for each grid point. Otherwise, grids with missing data were excluded in the analysis. Each complete time series was $Z$-transformed and used in the empirical orthogonal function (EOF) analysis.

EOF analysis was used to discern spatial and temporal patterns of wind stress curl and surface currents. EOF provides a compact description of the spatial and temporal variability of data series in terms of statistical "modes" (Emery & Thomson, 1997). Basically, the method involves the decomposition of a symmetric covariance matrix into its eigenvalues and eigenfunctions. EOF can be found by calculating the unitary eigenvectors of the covariance matrix associated with the sample data field (Chu et al., 1997). The time-dependent amplitudes and variance of the spatial modes are represented by the eigenvalues while spatial modes are represented by the eigenfunctions. A detailed description of EOF analysis can be found in Emery & Thomson (1997).

## RESULTS

Taking into account the annual monsoon cycle and the prevailing circulation over South China Sea, the statistical structure of wind stress curl and surface current fluctuations over the central basin were characterized. EOF analysis was utilized to determine dominant modes of variation for both data sets.

EOF analysis of the surface current field yields three dominant EOF modes. The top three modes account for 50%, 13%, and 7% of the total variance (Table 1). The temporal variations of the first three EOF modes for surface currents are shown in Fig. 2. Mode 1 remains constant throughout the year. The second and third modes represent seasonal variations with Mode 2 coinciding with the monsoon peaks (positive peak during June-August and negative peak during December-February), while Mode 3 peaks coincide with monsoon transition months (March-May and October).

The spatial variation of the temporally constant Mode 1 shows a weak eastward flow in the South China Sea and strong western boundary flow representing the Mindanao Current and Kuroshio Current east of Taiwan (Fig. 3). These features are generally persistent in the Pacific and exhibit relatively weak seasonality. Within the South China Sea, the strongest Mode 1 currents are found off the coast of Vietnam where the western boundary current system of the South China Sea exists.

Seasonality of surface circulation is evident in Mode 2, where the current exhibits an annual monsoonal cycle as seen in the variation of the temporal amplitude (Fig. 2). The amplitude is positive during the southwest monsoon season and negative during the northeast monsoon. The surface current Mode 2 spatial variation show the strongest currents in the South China Sea, specifically as a western boundary current extending from the southern part of the South China Sea to the coast off of Vietnam (Fig. 3). This western boundary current flows

Table 1. Eigenvalues of the EOF modes for surface currents and wind stress curl.

| Modes | Eigenvalue | Percent |
|---|---|---|
| Surface currents | | |
| 1 | 12.07 | 50% |
| 2 | 3.12 | 13% |
| 3 | 1.67 | 7% |
| Wind stress curl | | |
| 1 | 4.82 | 40% |
| 2 | 3.81 | 31% |

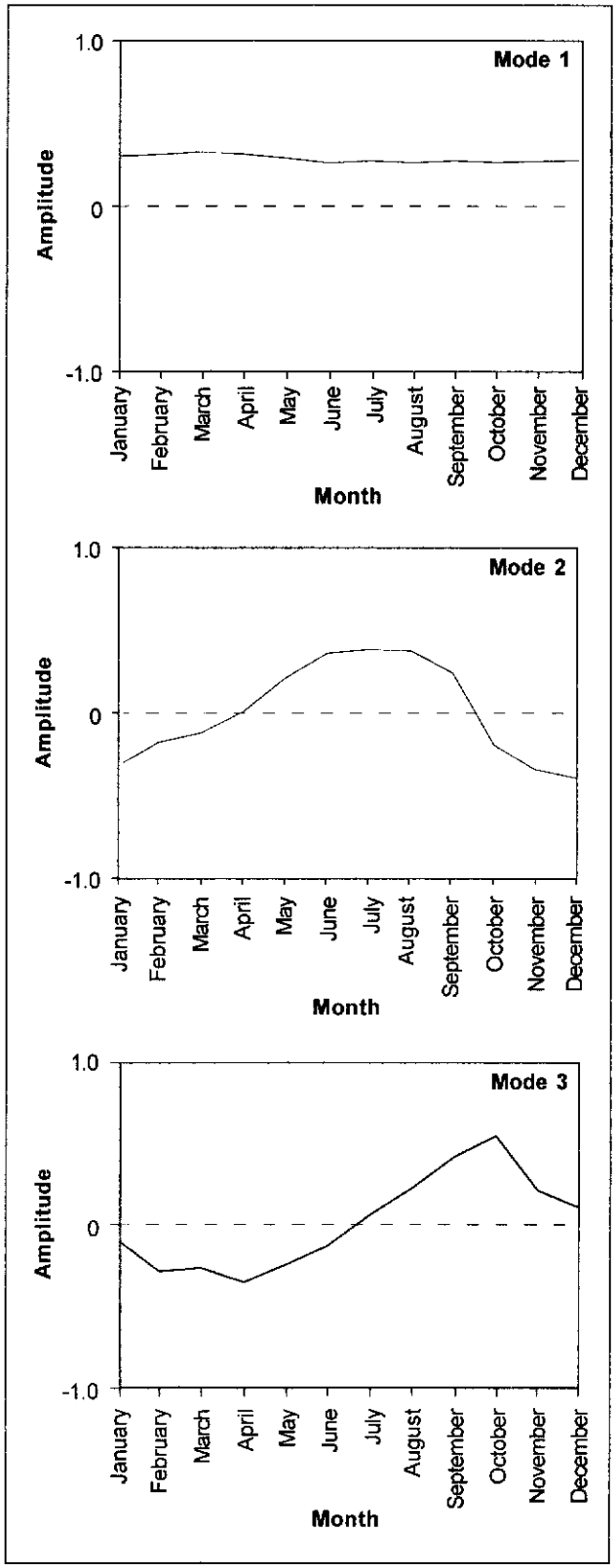


Fig. 2. Empirical orthogonal function (EOF) temporal amplitudes for surface currents Mode 1, Mode 2, and Mode 3.

northward during the southwest monsoon (positive amplitude) and reverses during the northeast monsoon (negative amplitude). In the interior, the surface currents reflect surface Ekman drift driven by the monsoons.

EOF Mode 3 represents surface circulation, which dominates during the monsoon transition periods. The temporal amplitude shown in Fig. 2 suggests that conditions during the spring transition are different from the autumn transition. However, it is also possible that this mode represents the dominance of the circulation in the Sulawesi Sea during the monsoon transition months. This is supported by the strong current magnitudes in the Sulawesi Sea for EOF Mode 3 spatial variation (Fig. 3).

EOF analysis of wind stress curl data yielded modes which unfortunately did not match the surface current modes in terms of its temporal scale. Mode 1 accounted for 40% of the variance (Table 1) and explains the positive wind stress curl distribution that dominates in the South China Sea and east of Mindanao (Fig. 4) during the northeast monsoon (Fig. 5). Previous studies suggest that the positive wind stress curl in the South China Sea drives a basin-wide upwelling (Chu et al., 1998), while the positive curl east of Mindanao drives the development of the Mindanao Dome (Masumoto et al., 1991; Udarbe & Villanoy, 2001). Mode 2 of wind stress curl, accounting for 31% of the total variance (Table 1), dominates during the southwest monsoon and divides the South China Sea into a positive wind stress curl in the north and a negative wind stress curl in the south. This wind stress curl distribution is consistent with the twin gyre circulation in the South China Sea during the southwest monsoon (Shaw et al., 1999).

## DISCUSSION

The South China Sea encompasses the largest body of semi-enclosed tropical water where circulation is driven by the annual reversal of monsoon winds. However, wind stress curl forcing is believed to be the dominant process controlling the circulation in the South China Sea (Wu et al., 1998; Shaw et al., 1999). Response of the upper layer circulation to the monsoonal wind is consistent with the large seasonal variations in the wind stress curl distribution, particularly in the southern half

of the South China Sea. The positive wind stress curl over the South China Sea during winter drives a predominantly cyclonic circulation. On the other hand, the presence of a positive wind stress curl in the north and a negative wind stress curl in the south result in the development of a dipole system during summer (Shaw et al., 1994).

Seasonal reversal of the South China Sea western boundary current dominates seasonal variations in the South China Sea. This is particularly evident in the southern part of the South China Sea up to the eastern coast of Vietnam and is consistent with the latitude range where wind stress curl variations result in a reversal of signs. The consistently negative wind stress curl in the northern South China Sea, coupled with strong winds from the northeast, intensifies the western boundary flow from the north to the south coast of Vietnam and reaches its maximum during December. As the northeast monsoon progresses, this western boundary current strengthens and extends southward. The western boundary current reverses during the summer monsoon. However, unlike the winter boundary current, which follows the western boundary throughout, the summer boundary current splits, separating from the coast off Vietnam and flows towards the east. The lateral boundary forcing is the major contributor to the formation of the strong western boundary current along southeast Chinese coast during winter, and the northward western boundary currents along Vietnamese coast during summer (Chu et al., 1998).

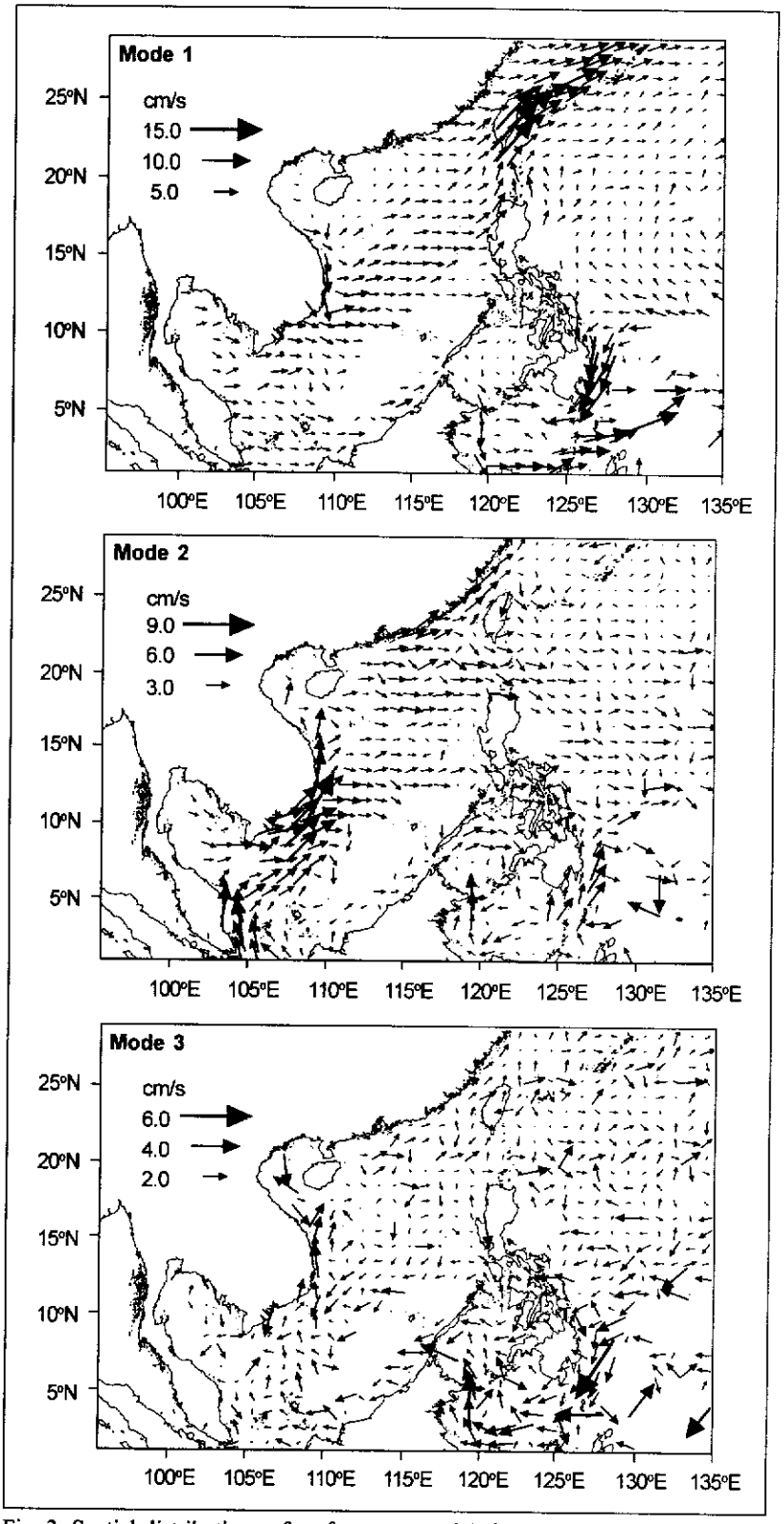


Fig. 3. Spatial distributions of surface currents Mode 1, Mode 2, and Mode 3.

The eastward flow corresponds to the lateral convergence of two areas of opposite curl signs, positive curl in the north and negative curl in the south with zero curl along a line from southern Vietnam to the

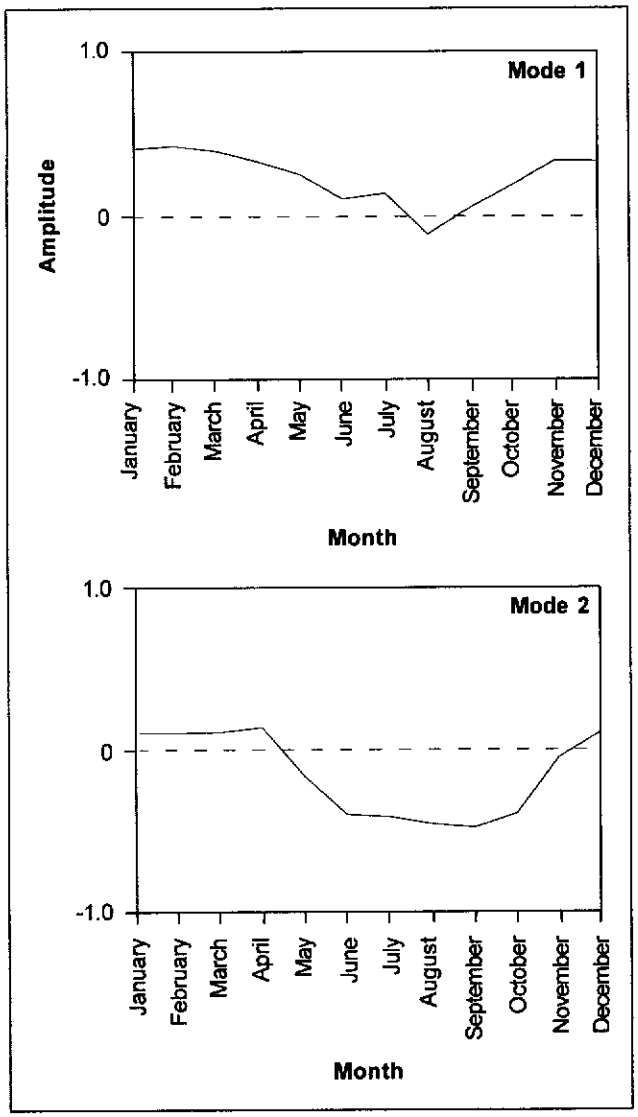


Fig. 4. Empirical orthogonal function (EOF) temporal amplitudes for wind stress curl Mode 1 and Mode 2.

Philippines. The line along which the curl is equal to zero provides natural boundaries that separate the circulation into gyres (Thurman, 1988). Unlike the previous modeling studies in the South China Sea which show the formation of distinct gyres, EOF analysis of surface currents reveal that most of the surface flow in the interior of the South China Sea outside the western boundary currents are mostly zonal. With the prevailing wind directions, this zonal flow seems to be associated with Ekman drift under northeast and southwest monsoons with the influence of the wind stress curl. The eastward current which forms the extension of the western boundary current during summer appears in the interior as the flow with the largest zonal component near the zero curl line.

It is not surprising that western boundary currents in the western Pacific stand out in the EOF analysis compared to the South China Sea western boundary currents (EOF Mode 1). The Western Pacific boundary current magnitudes are large by comparison because the western Pacific boundary currents are mainly driven by trade winds from the northeast and the North Equatorial Current (NEC). Before reaching the Philippine Islands, the NEC splits into the northern branch, which forms the origin of the Kuroshio, and a southern branch, which feeds the Mindanao Current. This occurs on the east of the Philippines where a definite division of the current takes place. The local circulation around the Philippines affects the transport of the Mindanao Current, as well as the bifurcation latitude of the NEC (Masumoto et al., 1991).

Despite the strong influence of the tradewinds, variations related to the monsoons may be evident in the Philippine Sea, particularly off Mindanao. This might be the explanation to the inconsistency in the temporal scale of the wind stress curl and surface current in Mode 1. The almost constant temporal variation of the surface current is due to the fact that there are no significant seasonal fluctuations in the transport of the Pacific western boundary current near the Philippine coast (Qui et al., 1996). For the EOF temporal amplitude of the wind stress curl, the pattern coincides with the generation of the Mindanao Dome off the Philippine coast, which evolves in late fall and reaches its maximum in late winter due to the positive curl associated with the northeast Asian winter monsoon that increases over the region (Masumoto & Yamagata, 1991). The temporal amplitude reverses in August, which is consistent with the weakening of the dome from early spring through early summer. EOF Mode 2 for the surface currents show strong seasonal variations associated with the Mindanao eddy. Richardson's ship-drift derived surface current data show a branch of the Mindanao Current flowing through the Celebes Sea and into Makassar Strait. A part of the Mindanao Current transport feeds the Indonesian throughflow, whose variability is also defined by the monsoons (Fine et al., 1994).

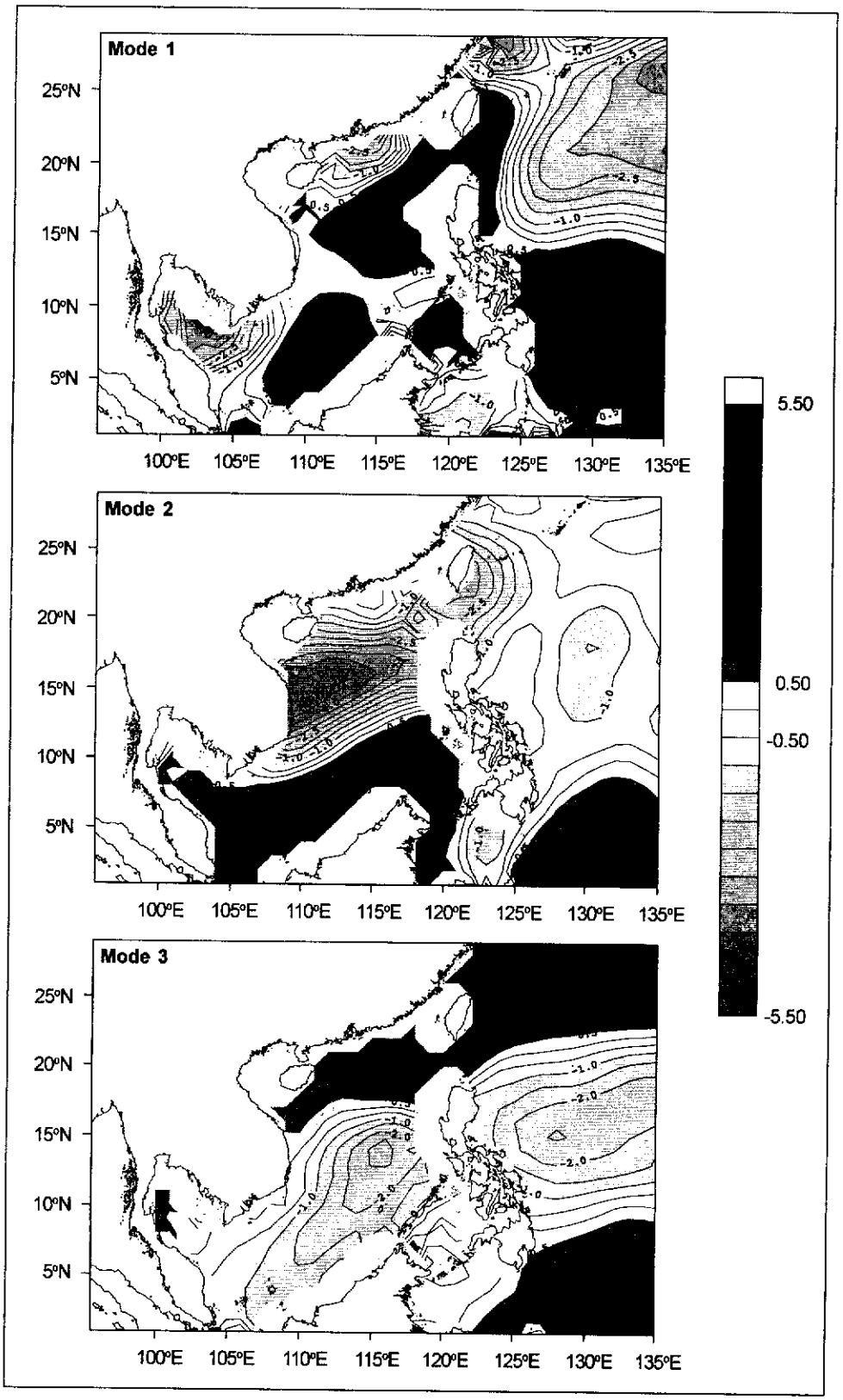


Fig. 5. Spatial structure of the first three wind stress curl modes. Contour intervals are $0.5 \times 10^{-7} Nm^{-3}$.

EOF analysis can derive precise mathematical descriptions and define modes of variations. This allows us to delineate the major modes having a large degree of spatial and temporal coherence between wind stress curl and surface circulation in the South China Sea. Three dominant EOFs account for almost 70% and 89% of the total variance of surface current and wind stress curl, respectively. Seasonal variations of wind stress curl contribute 72% of the total variance, while seasonal variations of the surface current only contributed 13 % of the variance for both the South China Sea and Philippine Sea. The small seasonal contribution is probably due to the dominance of the persistent western Pacific boundary currents. However, wind stress curl influences much of the surface circulation in the South China Sea, particularly along the western boundary currents. Since seasonal variability of wind stress curl is highest in the southern part of the South China Sea, large seasonal reversals dominate, particularly that of the western boundary flow. Meanwhile, in the interior of the South China Sea

and away from the western boundaries, surface current patterns are mainly due to Ekman drift.

## ACKNOWLEDGMENTS

The authors would like to thank the Philippine Council for Aquatic Marine Research and Development of the Department of Science and Technology (PCAMRD-DOST) for providing funding support; National Oceanic and Atmospheric Administration (NOAA) for access to the the datasets used in this study; Dr. Maria Jayvee Udarbe-Walker for the comments and suggestion; Jose de Leon for programming assistance; and to the research assistants in the Physical Oceanography Laboratory for their help and assistance. Finally, to the anonymous reviewers for their suggestions in improving the manuscript.

## REFERENCES

Chao, S.Y., P.T. Shaw, & S.Y. Wu, 1996. El Niño modulation of the South China Sea circulation. *Prog. Oceanogr.* 38: 51-93.

Chao, S.Y., P.T. Shaw, & C.R. Wu, 1998. Seasonal and inter-annual variations in the velocity field of the South China Sea. *J. Oceanogr.* 54: 361-372.

Chao, S.Y., P.T. Shaw, & J. Wang, 1995. Wind relaxation as a possible cause of the South China Sea warm current. *J. Oceanogr.* 51: 111-132.

Chu, P.C., S. Lu, & Y. Chen, 1997. Temporal and spatial variabilities of the South China Sea surface temperature anomaly. *J. Geophys. Res.* 102(C9): 20937- 20955.

Chu, P.C., Y. Chen, & S. Lu, 1998. Wind-driven South China Sea deep basin warm-core/cool-core eddies. *J. Oceanogr.* 54: 347-360.

Chu, P.C. & H.C. Tseng, 1997. South China Sea warm pool detected in spring. *Master Oceanographic Observational Data Set (MOODS).* 102(C7): 15761- 15771.

Emery, W.J. & R.E. Thomson, 1997. Data analysis methods in physical oceanography. New York, Elsevier Science, Inc.: 634 pp.

Fine, R.A., R. Lukas, F.M. Bingham, R.H. Gammon, & M.J. Warner, 1994. The western equatorial Pacific: A water mass crossroads. *J. Geophys. Res.* 99: 25063-25080.

He, Y., T. Yamagata, T. Guan, & Y. Masumoto, 1987. Seasonal changes in the South China Sea circulation (unpub.).

Masumoto, Y. & T. Yamagata, 1991.Response of the western tropical Pacific to the Asian winter monsoon: The generation of Mindanao dome. *J. Phys. Oceanogr.* 21: 1386-1398.

Qui, B. & R. Lukas, 1996. Seasonal and inter-annual variability of the north equatorial current, the Mindanao current, and the Kuroshio along the Pacific western boundary. *J. Geophys. Res. C.* 101(5): 12315-12330.

Qu, T., 2000. Upper-layer circulation in the South China Sea. *J. Phys. Oceanogr.* 30: 1450-1460

Pohlman, T.A., 1987. Three-dimensional circulation model of the South China Sea, three-dimensional models of marine and estuarine dynamics. *Elsevier Oceanography Series.* 45: 245-268.

Richardson, P.L. & T.K. McKee. (n.d.). Monthly climatology of ship-drift derived surface currents. Live access to reference data at PMEL. http://ferret.wrc.noaa.gov/las/main.pl. Accessed 1999 May.

Shaw, P.T. & S.Y. Chao, 1994. Surface circulation in South China Sea. *Deep Sea Res.* 41-I(11,12): 1663-1683.

Shaw, P.T., S.Y. Chao, & L.L. Fu, 1999. Sea surface height variations in the South China Sea from satellite altimetry. *Oceanologica. Acta.* 22(1): 1-17.

Shiver, J.F. & H.E. Hurlburt, 1997. The contribution of the global thermohaline circulation to the Pacific-to-Indian Ocean throughflow via Indonesia. *J. Geophys. Res. C.* 102(3): 5491-5511.

Thurman, H.V., 1988. Introductory oceanography. 6th ed. Ohio, Charles E. Merrill Publishing Company: 356 pp.

University of Wisconsin-Milwaukeen (UWM)/ Comprehensive ocean-atmosphere data set (COADS). (n.d.). Atlas of surface marine data 1994, served by National

Oceanographic Data Center (NOAA)/Pacific Marine Environmental Laboratory (PMEL). Live access to reference data at PMEL. http://ferret.wrc.noaa.gov/las/main.pl. Accessed 1999 May.

Wu, C.R., P.T., Shaw, & S.Y. Chao, 1998. Seasonal and inter-annual variations in the velocity field of the South China Sea. *J. Oceanogr.* 54: 361-372.

*Date received: January 7, 2003*
*Date accepted: July 9, 2003*